HHS Public Access

Author manuscript

J Tissue Eng Regen Med. Author manuscript; available in PMC 2018 February 12.

Published in final edited form as:

J Tissue Eng Regen Med. 2010 December ; 4(8): 590–599. doi:10.1002/term.268.

Development of an *in vitro* model to study the impact of BMP-2 on metastasis to bone

Heenam Kwon, **Hyeon Joo Kim**, **William L. Rice**, **Balajikarthick Subramanian**, **Sang-Hyug Park**, **Irene Georgakoudi**, and **David L. Kaplan***

Department of Biomedical Engineering, Tufts University, Medford, MA 02155, USA

Abstract

Prostate cancer cases and deaths have increased for years, yet the mechanisms involved in prostate cancer metastasis to bone remain poorly understood. To address this need, an effective and relevant *in vitro* model for the study of prostate cancer bone metastases would be useful. Therefore, a 3D *in vitro* tissue system was established using prostate cancer cells (PC3), suitable culture conditions and a 3D silk scaffold biomaterial to provide mechanically robust and slow degrading matrices to support the tissues for extended time frames. The role of BMP-2 on the progression of prostate cancer was investigated using this 3D tissue system. The results suggest that BMP-2 stimulates the migration of PC3 cells, suggesting insight into mechanisms involved in this critical step in the disease. The data support the conclusion that this *in vitro* system mimics aspects of prostate cancer metastasis in the presence of BMP-2, thus the system can be utilized as a starting point as an *in vitro* model for further studies of prostate cancer development and metastasis, as well as in the screening of new therapeutic treatments.

Keywords

prostate; cancer; metastasis; BMP-2; silk; PC3

1. Introduction

Prostate cancer has become the most commonly diagnosed cancer and the second leading cancer for death in men (Jemal *et al.*, 2008). According to the American Cancer Society (ACS), prostate cancer accounted for about 25% of newly diagnosed cancers in 2008 (Jemal *et al.*, 2008). Prostate cancer patients suffer from painful bone metastasis, which is the major cause of morbidity. Although the cancer cases and deaths continue to increase, the mechanisms of prostate cancer bone metastasis are poorly understood.

Most studies in prostate cancer have focused on the elucidation of mechanisms involved in prostate cancer metastasis to bone. The exchange of biological information between prostate cancer cells and the bone microenvironment are important in the establishment of bone metastasis (Yoneda and Hiraga, 2005). Thus, many researchers have investigated cell–cell

*Correspondence to: David L. Kaplan, Department of Biomedical Engineering, Tufts University, Medford, MA 02155, USA. david.kaplan@tufts.edu.

signalling pathways, such as Wnt (Hall *et al.*, 2005; Zhu *et al.*, 2004), dickkopf-1 (DKK-1) (Hall *et al.*, 2005), receptor activator of NF-κB ligand (RANKL) (Armstrong *et al.*, 2008; Zhang *et al.*, 2001), Noggin (Groppe *et al.*, 2002; Schwaninger *et al.*, 2007), matrix metalloproteinases (MMPs) (Madigan *et al.*, 2008; Nemeth *et al.*, 2002), and growth factor pathways in bone, such as transforming growth factors (TGFβ) (Sato *et al.*, 2008) and bone morphogenic proteins (BMPs) (Feeley *et al.*, 2005, 2006).

Aside from the mechanistic studies mentioned above, *in vivo* studies using animal models have also been pursued to gain insight into modes of prostate cancer formation and progression. Studies have included severe combined immunodeficient (SCID) mice (Nemeth *et al.*, 1999) and non-obese diabetic/severe combined immunodeficient (NOD/SCID) mice (Yonou *et al.*, 2001) to assess the behaviour of metastatic cancer cells. However, these animal models are difficult to use to study the molecular mechanisms involved in the process of metastasis due to various factors, such as issues of compatibility between implanted human fetal or adult bone in non-human carriers. Further, animal responses are not necessarily indicative of human responses; thus, links in outcomes have to be carefully considered.

Three-dimensional (3D) *in vitro* tissue culture systems have been introduced for cancer research, providing important insights into mechanisms involved in cancer metastasis (Mastro and Vogler, 2009; Kim *et al.*, 2004). The advantage of these 3D tissue culture systems is the ability to co-culture multiple cell types and recreate the 3D cancer and bone microenvironmens in bioreactors and rotary cell culture systems. These 3D *in vitro* cancer tissue systems have been used to demonstrate cell–cell interactions, intercellular adhesion and signalling between cells. However, 3D *in vitro* tissue culture systems are difficult to use to study cancer metastasis, such as migration and invasion.

The lack of relevant *in vitro* 3D models to study the mechanisms involved in prostate cancer metastasis presents a significant problem. Most studies *in vitro* for prostate cancer have been conducted with two-dimensional (2D) cell cultures. These cultures have included a range of prostate cancer cells, including PC3, LNCaP and DU145, for the study of cell signalling pathways involved in bone metastasis (Brubaker *et al.*, 2004; Mori *et al.*, 2007). Although 2D cultures are fundamental in many studies and provide useful information, the use of 3D models *in vitro* is necessary in terms of the improved relevance to cellular function and for tissue structure and function. Furthermore, 3D systems can be studied with more consistency than *in vivo* models in terms of controlling the inputs and outputs, such as cell types, cell numbers and matrix details. Thus, 3D systems provide better statistical interpretation and are valuable for the study of mechanisms.

For 3D tissue culture systems, aside from the cell components, the matrix or biomaterial plays a critical role in supporting cell functions, transport and overall system feasibility. Silk-based biomaterials have previously been used to provide benefits over conventional synthetic degradable polymers (e.g. polyglycolic and lactic acid co-polymers) and natural polymers (e.g. collagen type I) in generating mesenchymal tissues such as bone, cartilage and ligaments (Wang *et al.*, 2006). Silks have good biocompatibility, slow degradation rates and impressive mechanical properties (Altman *et al.*, 2003) that can address the need for

biomedical and biotechnological applications, such as the formation of sustainable and functional 3D tissue architectures. We have also previously demonstrated this utility in the study of human breast cancer metastasis with the use of 3D porous silk scaffolds for the formation of human bone implants (Moreau *et al.*, 2007). The surfaces of silk fibroin can also be modified through various chemical processes by decorating with bone morphogenic protein (BMP-2) or adhesion peptides such as RGD (Karageorgiou *et al.*, 2004; Sofia *et al.*, 2001) to enhance osteogenic differentiation and cell attachment, respectively. The modification of silk surfaces with various gradients of factors, such as via microvesicle delivery, can provide new biomaterials and help towards the formation of different and more complex types of structures, such as osteochrondral systems (Wang *et al.*, 2009).

Bone morphogenic proteins (BMPs) are members of the transforming growth factor-β (TGFβ) superfamily (Hogan, 1996) and a major group of cell signalling factors that induce bone formation (Bobinac *et al.*, 2005). BMPs have been suggested to have a significant role in the formation of osteoblastic lesions caused by prostate cancer metastasis (Feeley *et al.*, 2005). BMP receptors have also been detected in prostate cell lines such as LNCaP and PC3 (Ide *et al.*, 1997). BMP-2, one of the BMP family members, has been demonstrated to be involved in osteoblast lineage differentiation (Yamaguchi *et al.*, 1991) and has the ability to induce new bone formation (Wozney, 1992). Prostate cancer typically metastasizes to bone and BMP-2 has been found expressed in prostate cancer cells with established bone metastases (Bobinac *et al.*, 2005). Therefore, the role of BMP-2 on the progression of prostate cancer is suggested to be an important factor in the study of bone metastases.

The aim of the present study was to establish a new sustainable 3D tissue system to mimic the metastasis of prostate cancer *in vitro* and then to utilize this system to understand mechanisms of prostate cancer metastasis. Silk fibroin scaffolds were used in the 3D model system because of their functional features, outlined above. In the present study, we demonstrated an initial *in vitro* system towards a prostate cancer metastasis tissue model system. As a first step we observed, in particular, the effect of BMP-2 on the process of metastasis. Although the present study does not include tissue-engineered bone to mimic the metastasis of prostate cancer, the study suggests that the *in vitro* system is effective and relevant towards further studies of prostate cancer metastasis.

2. Materials and methods

2.1. Preparation of silk scaffolds

Aqueous-based silk scaffolds were prepared according to our previously described procedures (Kim *et al.*, 2005). Briefly, cocoons of *Bombyx mori* were boiled for 20 min in an aqueous solution of 0.02 M Na_2CO_3 and rinsed with distilled water to eliminate sericin. Purified silk fibroin was solubilized in 9.3 M LiBr solution and dialysed against distilled water to generate a solution of 8 w/v% silk. The silk solution obtained was used to generate the scaffolds by adding 4 g NaCl (particle size, 1000–1180 μm) into 2 ml silk solution in disk-shaped containers at room temperature. Twenty-four hours later the containers were immersed in distilled water to extract the salt from the porous scaffolds over 2 days. The scaffolds were cut into 8 × 3 mm (diameter × height) discs and autoclaved in preparation for cell seeding.

2.2. Cell culture on silk scaffolds

The human prostate cancer cell line PC3 from the American Type Culture Center (Manassas, VA, USA) was used for the experiments. PC3 cells were cultured in DMEM/F12 (Gibco, Carlsbad, CA, USA) with 10% FBS, 100 U/ml penicillin, 100 μg/ml streptomycin and 0.25 μg/ml fungizone. PC3 (2×10^6 cells/scaffold) was seeded onto scaffolds pre-wetted with DMEM/F12 overnight and placed in a humidified tissue culture incubator at 37 °C with 5% CO_2 for 2 h to allow the cells to attach. The scaffolds seeded with PC3 cells were maintained in the same medium as used in PC3 cell culture and incubated for 1 day before evaluation. The 3D cell migration systems I and II described below were maintained in tissue culture wells with 11 ml medium.

2.3. Labelling PC3 with DiI

A solution of DiI (diakylcarbocyanine: D-282, Molecular Probes, USA) in culture medium was prepared by diluting a 2.5 mg/ml stock solution in ethanol to a final concentration of 10 μM. Cell suspensions were incubated with the loading solution for 30 min at 37 °C. After loading, the cells were spun down and resuspended in fresh medium.

2.4. 3D cell migration system I

Aqueous-based silk fibroin scaffolds with a pore size distribution of 1000–1180 μm, with interconnected pores and overall scaffold dimensions of 8 mm diameter and 3 mm height were prepared as previously described (Kim *et al.*, 2005) (Figure 1B, C). Two scaffolds were attached to each other to track the migration of prostate cancer cells from the top scaffold to the bottom scaffold. A needle (23 gauge, Precision Glide, Becton Dickinson & Co, Franklin Lakes, NJ, USA) was used to hold the two scaffolds together and was attached to a bottom rubber matt (silicon rubber; McMaster-Carr, Robbinsville, NJ, USA) to hold the samples in place in tissue culture wells during growth in the medium (Figure 1A). The top scaffolds were seeded with the prostate cancer cell line PC3. Each scaffold seeded with cells was incubated for 1 day separately before evaluation. The migration of PC3 cells to the bottom scaffolds was studied under two different conditions; unmodified scaffolds and BMP-2-coupled scaffolds. PC3 cell migration in the presence or absence of BMP-2 was characterized by confocal microscopy, RT–PCR and histology.

2.5. 3D cell migration system II

The 3D model system designed by organizing the two scaffolds vertically can be impacted by gravitational influences on the cell migration assays. Thus, to avoid this impact, an alternative system was utilized in which we further examined the effect of BMP-2 on cell migration by placing the scaffolds seeded with PC3 cells on the bottom side in the *in vitro* system and observing the migration of the cells into the top scaffolds. The migration of PC3 cells to the top scaffolds was determined by measuring the DNA content in the scaffolds.

2.6. Confocal and two-photon excited Fluorescence microscopy

Migration of DiI-labelled PC3 cells was examined qualitatively by their distribution in the bottom scaffolds after specified time points. The bottom scaffolds were processed prior to imaging by washing once with PBS. Fluorescence images were acquired on a Leica

DMIRE2 microscope with a TCS SP2 scanner (Wetzlar, Germany) through a ×20 (NA 0.7) air objective. Samples were placed on culture dishes with number 1.5 cover glass bottoms (Mattek, Ashland, MA, USA) and the fluorescence emission was collected with either single-photon excitation for visualizing labelled cells, at 543 nm and confocal detection over a spectral range of 550–575 nm, or with two-photon excitation for visualizing the silk scaffolds. The latter was with a Mai Tai titanium sapphire laser tuned to 800 nm, emitting 100 fs pulses at 80 MHz (Spectra Physics, Mountain View, CA, USA) and a filter cube containing a 700 nm short-pass filter (Chroma SPC700 bp) a dichroic mirror (Chroma 495dcxr) and emitter bandpass filters centred at 455 nm (Chroma 455bp70). Analysis was performed using Leica Confocal software (Wetzlar, Germany) and ImageJ (NIH).

2.7. BMP-2 coupling

BMP-2 was generously provided by Wyeth Bio-Pharmaceuticals (Andover, MA, USA) or purchased from R&D Systems (Minneapolis, MN, USA). BMP-2 solution was sterilized through 0.22 μm syringe filters (Millipore, Billerica, MA, USA). Activation buffer 4-morpholinoethanesulphonic acid (MES) buffer (Pierce, Woburn, MA, USA) was prepared according to the manufacturer's instructions, MES 0.1 M plus NaCl 0.5 M adjusted to pH 6 and sterilized by using 0.22 μm syringe filters. The scaffolds were immersed in excess MES buffer with 1-ethyl-3-(3-dimethylaminopropyl) carbodiimide hydrochloride (EDC)/*N*-hydroxysuccinimide (NHS) (10/15 mg in 20 ml) for 15 min. The buffer was then removed and the scaffolds washed with MES buffer without EDC/NHS. BMP-2 solution (30 μg/scaffold) was added onto the scaffolds and allowed to react for 2 h. Then the scaffolds were washed twice with PBS. To assess concentrations of BMP-2, culture medium was collected for quantification of removed BMP-2 from the scaffolds, using an ELISA kit assay according to the manufacturer's instructions (Quantikine; R&D Systems, Minneapolis, MN, USA).

2.8. Biochemical analysis

To determine the migration of PC3 cells to the top scaffolds using 3D cell migration system II, the top scaffolds were chopped with microscissors on ice and the DNA content in the scaffolds were measured by Picogreen assay (Molecular Probes, Eugene, OR, USA), according to the manufacturer's protocol. The samples were measured fluorometrically at excitation/emission = 480/528 nm.

2.9. RNA isolation and real-time RT–PCR

Scaffolds were transferred to 2 ml plastic tubes and 1 ml Trizol was added. The scaffolds were chopped with microscissors and the tubes were centrifuged (12 000 × *g*) for 10 min. The supernatant was transferred to new tubes and 200 ml chloroform was added to the solution. The tubes were centrifuged at 12 000 × *g*) for 15min, the upper aqueous phase was transferred to a new tube and one volume of 70% ethanol was added to the tubes. RNA was obtained using the RNeasy minikit (Qiagen, Hilden, Germany) according to the manufacturer's protocol. The RNA was reverse-transcribed into cDNA, using oligo (dT)-selection, according to the manufacturer's protocol (High Capacity cDNA Archive Kit, Applied Biosystems, Foster City, CA, USA). Gene expression of collagen type I, osteocalcin, DKK-1, Noggin, Wnt 7B and pS2 were quantified using the ABI Prism 7000

Real-time PCR System (Applied Biosystems, Foster City, CA, USA) for 2 min at 50 °C, 10 min at 95 °C, 50 cycles at 95 °C for 15 s and 1 min at 60 °C. The transcript levels were normalized to glyceraldehyde 3-phosphate dehydrogenase (GAPDH).

2.10. Histology

Specimens were fixed with 10% buffered formalin phosphate for at least 24 h, embedded in paraffin and sectioned at 5 μm. Serial sections were stained with haematoxylin and eosin (H&E) according to standard histochemical techniques.

2.11. Statistics

Statistical analysis of data was performed by *t*-tests with a minimum of three samples. $*p < 0.05$ and $**p < 0.01$ were considered statistically significant.

3. Results

3.1. Quantification of BMP-2 by ELISA

The BMP-2 concentration recovered from the scaffolds was determined by ELISA. The amount of BMP-2 initially loaded onto the scaffolds was 30 μg. After 2 days, ~60 ng/ml BMP-2 was removed from the scaffolds in the 3D cell migration system I. When the amount of BMP-2 covalently coupled to the scaffolds was maximal, 30 μg, 2.2% (660 ng/11 ml) of the initial amount of BMP-2 was removed from the scaffolds after 2 days and BMP-2 continued to be recovered at low levels (Figure 2). BMP-2 removed from the scaffolds in the 3D cell migration system II was ~650 ng/ml, which was 23.8% (7.15 μg/11 ml) of the initial amount of BMP-2 after 2 days (Figure 7B).

3.2. Confocal microscopy

PC3 cells labelled with DiI were seeded on silk scaffolds (Figure 3) and placed on the top layer in the *in vitro* system. The migration of PC3 cells to the bottom scaffolds was determined based on the presence or absence of BMP-2. Scaffolds before evaluation were used as a control and denoted as day 0. PC3 cells were found in the bottom scaffolds cultured for 2 days by tracking with confocal microscopy (Figure 4). The images were collected from the top sides (~150 μm inside) of the bottom scaffolds where they met with the top scaffolds. Cells were tracked in the scaffolds based on the presence of fluorescence emission due to labelling with DiI. Using this approach, the distribution of PC3 cells was found to be similar in the unmodified and BMP-2-coupled scaffolds.

3.3. Gene expression in the bottom scaffolds

Transcript expression of several markers, including collagen type I (Col I), osteocalcin (OC), Wnt 7B, dickkopf-1 (DKK-1), pS2 and Noggin, were quantified. After 2 days of incubation, all transcript levels were significantly increased in the BMP-2-coupled scaffolds when compared with the unmodified silk scaffolds (Figure 5).

3.4. Histological examination

Histological examination of the bottom scaffolds using H&E staining showed that the PC3 cells were present in the sectioned bottom scaffolds, which were unmodified silk scaffolds and BMP-2-coupled scaffolds, after 2 days of incubation (Figure 6B, D). Scaffolds before evaluation were used as a control (Figure 5A, C).

3.5. Biochemical analysis

The migration of PC3 cells to the top scaffolds in the presence or absence of BMP-2, using 3D cell migration system II, was determined by measuring the DNA content. After 2 days the DNA content in the BMP-2-coupled scaffolds was significantly higher than the concentration in the unmodified scaffolds (Figure 7). This result suggests that more PC3 cells from the bottom scaffolds migrated into the top scaffolds in the presence of BMP-2 when compared to the unmodified scaffolds.

4. Discussion

Bone metastases from prostate cancer are predominantly characterized as osteoblastic. One hypothesis is that the osteoblastic lesions are established with underlying osteolytic lesions (Morrissey and Vessella, 2007). Prostate cancer cells produce osteolytic factors, resulting in the release of growth factors from bone, which eventually induces bone production and causes these osteoblastic lesions (Hall *et al.*, 2006; Morrissey and Vessella, 2007). Based on this hypothesis, in the present study we focused on the osteolytic phase of this process. Thus, for the present study we selected the PC3 osteolytic cell line derived from bone metastasis that exhibits an osteolytic phenotype in bone (Logothetis and Lin, 2005). BMP-2 is suggested to be a significant factor in the progression of prostate cancer, due to its expression in prostate cancer cells with established bone metastasis (Bobinac *et al.*, 2005). A 3D *in vitro* model system using 3D silk fibroin scaffolds was established in the present study to investigate the role of BMP-2 in prostate cancer metastasis. The migration of PC3 cells seeded from one set of scaffolds to the other was determined based on the presence or absence of BMP-2.

Gene expression by PC3 cells in scaffolds coupled with BMP-2 showed significant increases when compared to transcript expression in the unmodified silk scaffolds, suggesting stimulation when the cells were exposed to BMP-2. Osteogenic marker expression (Col I, OC) and Wnt 7B expression in the cells supported the hypothesis that prostate cancer cells have bone cell-like properties to survive, proliferate, migrate and invade the bone environment, as previously suggested (Koeneman *et al.*, 1999).

Wnt is a large family of proteins that mediate bone development and promote bone production (Hall and Keller, 2006). Wnt 7B activates the canonical signalling pathway in osteoblasts and has been suggested to be strongly involved in prostate cancer bone metastasis and contribute to the phenotype of bone metastasis by altering the balance between Wnt 7B and DKK-1 expression (Li *et al.*, 2008). Increased expression of Wnt 7B by the PC3 cells in the BMP-2-coupled scaffolds suggests that the expression may be stimulated when introduced into bone, and the increased signalling may contribute to

determining the phenotype of bone metastasis. DKK-1 and Noggin are antagonists of Wnt and BMP and are highly expressed in osteolytic prostate cancer cell lines (Schwaninger *et al.*, 2007). It has been shown that a lack of DKK-1 in osteolytic cell lines results in an osteoblastic phenotype (Hall *et al.*, 2005) and overexpression of Noggin in osteoblastic cell lines results in the abolition of the osteoblastic response *in vivo* (Schwaninger *et al.*, 2007). This suggests a significant role in determining the characteristic phenotype of bone metastasis. In the present study, increased transcript level of DKK-1 and Noggin when exposed to BMP-2 suggests that their osteolytic activity in the cells may be promoted when they meet with the bone environment, and their activity may be significant to determine the phenotype of bone lesions in the process of bone metastasis.

pS2 is highly expressed in prostate cancer cell lines and its protein expression has been found in prostate cancer tissues (Bonkhoff *et al.*, 1995; Cheung *et al.*, 2005). Prostatic differentiation markers such as prostate-specific antigen (PSA) and kallikrein 2 (hK2) are expressed in osteoblastic prostate cancer cell lines, and pS2 is expressed in both osteoblastic and osteolytic prostate cancer cell lines (Cheung *et al.*, 2005). Thus, pS2 may be used as a marker for osteolytic lesions caused by osteolytic bone metastasis. pS2 expression by the PC3 cells increased upon exposure to BMP-2, which suggests they are stimulated by interaction with the bone environment. Thus, this gene may be a useful marker to determine the phenotype of bone lesions and trace the process of bone metastasis established with underlying osteolytic lesions.

The 3D cell migration system I may introduce gravitational effects on cell migration. As shown by confocal microscopy and histology on the unmodified bottom scaffolds, similar features were found with BMP-2-coupled scaffolds, suggesting this possibility. Therefore, the migration of PC3 cells in system II, which placed the PC3 cells on the bottom, was used to eliminate this effect. Since the DNA content in the BMP-2-coupled scaffolds was significantly higher than those in the unmodified scaffolds, the data suggest that gravitational influence was not responsible for the outcomes with system I. Since BMP-2 does not influence the proliferation of PC3 cells (Brubaker *et al.*, 2004; Ide *et al.*, 1997), the increase in cell content in the BMP-2-coupled scaffolds can be explained based on cell migration.

In the 3D systems I and II, BMP-2 concentrations recovered from the BMP-2-coupled scaffolds after 2 days of incubation were 2.2% and 23.8%, respectively, of the initial amount of BMP-2 loaded. BMP-2 used in each system was obtained from different sources; thus, the activity is different and leads to differences in the BMP-2 concentrations recovered in each system. We have previously demonstrated that BMP-2 was covalently coupled on silk fibroin material using EDC/NHS coupling agents, and over 80% of the immobilized BMP-2 on the silk material was retained for 1 week and 50% of the amount of BMP-2 was retained on the material by 4 weeks (Karageorgiou *et al.*, 2004). In the present study, BMP-2 solubilized into the medium at a low level compared to the total delivered on the scaffolds through chemical coupling or via adsorption. Thus, there was still considerable immobilized BMP-2 on the scaffolds available to impact the cells. Feeley *et al.* (2006) performed a migration assay with PC3 cells to quantify the effect of BMP-2 and found a significant effect on PC3 cell migration at 100 ng/ml and 500 ng/ml, but not at lower concentrations (1 ng/ml

or 10 ng/ml). In this prior study, cells were migrating through a transwell system, unlike the system in the present study; thus, direct comparisons are not possible. However, their results suggest that prostate cancer cells are affected by BMP-2 at certain concentrations, and thus migrate toward bone. In the present study, based on the initially loaded BMP-2, the amount of retained BMP-2 on the scaffolds was significantly higher than the 100 ng/ml that was found effective in promoting cell migration in the prior study cited above (Feeley *et al.*, 2006). Thus, the amount of retained BMP-2 on the scaffolds was sufficient to affect the migration of PC3 cells in our system. We have also previously reported that silk fibroin 3D scaffolds with adsorbed BMP-2 initially released 75% of the loaded amount after 1 week (Karageorgiou *et al.*, 2006). Thus, the BMP-2 lost from the scaffolds in both systems is most likely due to the BMP-2 that was non-specifically adsorbed, as we have previously discussed (Karageorgiou *et al.*, 2006).

Transwell chambers have been used in prostate cancer studies to observe migration and invasion of cells under certain conditions and to study secreted factors or changes in gene expression though indirect cell–cell interactions (Moro *et al.*, 2008; Nabha *et al.*, 2008). Co-cultivation of two types of cells has been used for the study of direct cell–cell interaction. We have previously reported that osteoblasts stimulate the osteogenic differentiation of mesenchymal stem cells (MSCs) through the Wnt signalling pathway, and the effects were distinctive when cell–cell contact was direct or indirect (e.g. transwell) (Wang *et al.*, 2007). The present 3D *in vitro* system can provide both direct (e.g. physical contact) and indirect (e.g. use of a barrier) architectures for cell–cell interactions as well as 3D environments for cell growth; thus, this system can provide a valuable tool for the study of cell signalling involved in prostate cancer metastasis to bone.

There have also been many *in vivo* studies of prostate cancer using animal models with implanted human fetal or adult bone, to observe the migration of prostate cancer cells toward the bone following injection of the cells through the tail vein or in the prostate of mice (Singh and Figg, 2005; Singh *et al.*, 2006). However, these studies are difficult to utilize for the study of molecular mechanisms involved in this process, due to various confounding factors with animals. Further, these are not human systems. Our 3D *in vitro* system provides advantages, in that the processes involved can be studied more consistently and systematically than in *in vivo* models, due to the ability to control the inputs and outputs to and from the system. This leads to improved statistical outputs as well.

3D scaffolds using various biomaterials have been used in tissue engineering to support the formation of engineered tissues and to promote cellular functions. We have previously reported the use of 3D aqueous-based silk fibroin scaffolds for bone tissue engineering (Kim *et al.*, 2005, 2007). Human bone marrow mesenchymal stem cells (hMSCs) were grown in silk scaffolds under the appropriate differentiation conditions to generate tissue-engineered bone (Kim *et al.*, 2005, 2007). This tissue-engineered bone can serve as a 3D model system to support the migration and invasion of prostate cancer cells, as well as supporting tumour formation *in vitro*. These interactions between engineered bone and prostate cancer cells *in vitro* could be observed during the process of metastasis and the migration and invasion of prostate cancers, and tumour formation in the engineered bone could be characterized.

5. Conclusion

The lack of relevant *in vitro* tissue systems of prostate cancer metastasis to bone is a significant problem in current prostate cancer research. We report a first step towards the development of a suitable 3D *in vitro* tissue system for the study of prostate cancer metastasis. With this tissue system, the impact of BMP-2 on the progression of prostate cancer cells was demonstrated. A practical strategy utilizing a 3D model *in vitro* will support further studies of prostate cancer metastasis and provide an approach toward the development of screening methods for new drugs and therapies related to this disease.

Acknowledgments

We thank the NIH Tissue Engineering Resource Center (Grant No. P41 EB002520) for support of these studies.

References

Altman GH, Diaz F, Jakuba C, et al. Silk-based biomaterials. Biomaterials. 2003; 24(3):401–416. [PubMed: 12423595]

Armstrong AP, Miller RE, Jones JC, et al. RANKL acts directly on RANK-expressing prostate tumor cells and mediates migration and expression of tumor metastasis genes. Prostate. 2008; 68(1):92–104. [PubMed: 18008334]

Bobinac D, Maric I, Zoricic S, et al. Expression of bone morphogenetic proteins in human metastatic prostate and breast cancer. Croat Med J. 2005; 46(3):389–396. [PubMed: 15861517]

Bonkhoff H, Stein U, Welter C, et al. Differential expression of the pS2 protein in the human prostate and prostate cancer: association with premalignant changes and neuroendocrine differentiation. Hum Pathol. 1995; 26(8):824–828. [PubMed: 7635445]

Brubaker KD, Corey E, Brown LG, et al. Bone morphogenetic protein signaling in prostate cancer cell lines. J Cell Biochem. 2004; 91(1):151–160. [PubMed: 14689587]

Cheung CP, Yu S, Wong KB, et al. Expression and functional study of estrogen receptor-related receptors in human prostatic cells and tissues. J Clin Endocrinol Metab. 2005; 90(3):1830–1844. [PubMed: 15598686]

Feeley BT, Gamradt SC, Hsu WK, et al. Influence of BMPs on the formation of osteoblastic lesions in metastatic prostate cancer. J Bone Miner Res. 2005; 20(12):2189–2199. [PubMed: 16294272]

Feeley BT, Krenek L, Liu N, et al. Overexpression of noggin inhibits BMP-mediated growth of osteolytic prostate cancer lesions. Bone. 2006; 38(2):154–166. [PubMed: 16126463]

Groppe J, Greenwald J, Wiater E, et al. Structural basis of BMP signalling inhibition by the cystine knot protein Noggin. Nature. 2002; 420(6916):636–642. [PubMed: 12478285]

Hall CL, Bafico A, Dai J, et al. Prostate cancer cells promote osteoblastic bone metastases through Wnts. Cancer Res. 2005; 65(17):7554–7560. [PubMed: 16140917]

Hall CL, Kang S, MacDougald OA, et al. Role of Wnts in prostate cancer bone metastases. J Cell Biochem. 2006; 97(4):661–672. [PubMed: 16447163]

Hall CL, Keller ET. The role of Wnts in bone metastases. Cancer Metast Rev. 2006; 25(4):551–558.

Hogan BL. Bone morphogenetic proteins in development. Curr Opin Genet Dev. 1996; 6(4):432–438. [PubMed: 8791534]

Ide H, Yoshida T, Matsumoto N, et al. Growth regulation of human prostate cancer cells by bone morphogenetic protein-2. Cancer Res. 1997; 57(22):5022–5027. [PubMed: 9371496]

Jemal A, Siegel R, Ward E, et al. Cancer statistics. CA Cancer J Clin. 2008; 58(2):71–96. [PubMed: 18287387]

Karageorgiou V, Meinel L, Hofmann S, et al. Bone morphogenetic protein-2 decorated silk fibroin films induce osteogenic differentiation of human bone marrow stromal cells. J Biomed Mater Res A. 2004; 71(3):528–537. [PubMed: 15478212]

Karageorgiou V, Tomkins M, Fajardo R, et al. Porous silk fibroin 3D scaffolds for delivery of bone morphogenetic protein-2 *in vitro* and *in vivo*. J Biomed Mater Res A. 2006; 78(2):324–334. [PubMed: 16637042]

Kim HJ, Kim UJ, Leisk GG, et al. Bone regeneration on macroporous aqueous-derived silk 3D scaffolds. Macromol Biosci. 2007; 7(5):643–655. [PubMed: 17477447]

Kim HJ, Kim UJ, Vunjak-Novakovic G, et al. Influence of macroporous protein scaffolds on bone tissue engineering from bone marrow stem cells. Biomaterials. 2005; 26(21):4442–4452. [PubMed: 15701373]

Kim JB, Stein R, O'Hare MJ. Three-dimensional *in vitro* tissue culture models of breast cancer – a review. Breast Cancer Res Treat. 2004; 85(3):281–291. [PubMed: 15111767]

Kim UJ, Park J, Kim HJ, et al. Three-dimensional aqueous-derived biomaterial scaffolds from silk fibroin. Biomaterials. 2005; 26(15):2775–2785. [PubMed: 15585282]

Koeneman KS, Yeung F, Chung LW. Osteomimetic properties of prostate cancer cells: a hypothesis supporting the predilection of prostate cancer metastasis and growth in the bone environment. Prostate. 1999; 39(4):246–261. [PubMed: 10344214]

Li ZG, Yang J, Vazquez ES, et al. Low-density lipoprotein receptor-related protein 5 (LRP5) mediates the prostate cancer-induced formation of new bone. Oncogene. 2008; 27(5):596–603. [PubMed: 17700537]

Logothetis CJ, Lin SH. Osteoblasts in prostate cancer metastasis to bone. Nat Rev Cancer. 2005; 5(1): 21–28. [PubMed: 15630412]

Madigan MC, Kingsley EA, Cozzi PJ, et al. The role of extracellular matrix metalloproteinase inducer protein in prostate cancer progression. Cancer Immunol Immunother. 2008; 57(9):1367–1379. [PubMed: 18273614]

Mastro AM, Vogler EA. A three-dimensional osteogenic tissue model for the study of metastatic tumor cell interactions with bone. Cancer Res. 2009; 69(10):4097–4100. [PubMed: 19435905]

Moreau JE, Anderson K, Mauney JR, et al. Tissue-engineered bone serves as a target for metastasis of human breast cancer in a mouse model. Cancer Res. 2007; 67(21):10304–10308. [PubMed: 17974972]

Mori K, Le Goff B, Charrier C, et al. DU145 human prostate cancer cells express functional receptor activator of NFκB: new insights in the prostate cancer bone metastasis process. Bone. 2007; 40(4): 981–990. [PubMed: 17196895]

Moro L, Arbini AA, Yao JL, et al. Loss of BRCA2 promotes prostate cancer cell invasion through up-regulation of matrix metalloproteinase-9. Cancer Sci. 2008; 99(3):553–563. [PubMed: 18167127]

Morrissey C, Vessella RL. The role of tumor microenvironment in prostate cancer bone metastasis. J Cell Biochem. 2007; 101(4):873–886. [PubMed: 17387734]

Nabha SM, dos Santos EB, Yamamoto HA, et al. Bone marrow stromal cells enhance prostate cancer cell invasion through type I collagen in an MMP-12 dependent manner. Int J Cancer. 2008; 122(11):2482–2490. [PubMed: 18324629]

Nemeth JA, Harb JF, Barroso U Jr, et al. Severe combined immunodeficient-hu model of human prostate cancer metastasis to human bone. Cancer Res. 1999; 59(8):1987–1993. [PubMed: 10213511]

Nemeth JA, Yousif R, Herzog M, et al. Matrix metalloproteinase activity, bone matrix turnover, and tumor cell proliferation in prostate cancer bone metastasis. J Natl Cancer Inst. 2002; 94(1):17–25. [PubMed: 11773278]

Sato S, Futakuchi M, Ogawa K, et al. Transforming growth factor-β derived from bone matrix promotes cell proliferation of prostate cancer and osteoclast activation-associated osteolysis in the bone microenvironment. Cancer Sci. 2008; 99(2):316–323. [PubMed: 18271931]

Schwaninger R, Rentsch CA, Wetterwald A, et al. Lack of noggin expression by cancer cells is a determinant of the osteoblast response in bone metastases. Am J Pathol. 2007; 170(1):160–175. [PubMed: 17200191]

Singh AS, Figg WD. *In vivo* models of prostate cancer metastasis to bone. J Urol. 2005; 174(3):820–826. [PubMed: 16093963]

Singh AS, Macpherson GR, Price DK, et al. Evaluation of human fetal bone implants in SCID mice as a model of prostate cancer bone metastasis. Oncol Rep. 2006; 15(3):519–524. [PubMed: 16465406]

Sofia S, McCarthy MB, Gronowicz G, et al. Functionalized silk-based biomaterials for bone formation. J BiomedMater Res. 2001; 54(1):139–148.

Wang X, Wenk E, Zhang X, et al. Growth factor gradients via microsphere delivery in biopolymer scaffolds for osteochondral tissue engineering. J Control Release. 2009; 134(2):81–90. [PubMed: 19071168]

Wang Y, Kim HJ, Vunjak-Novakovic G, et al. Stem cell-based tissue engineering with silk biomaterials. Biomaterials. 2006; 27(36):6064–6082. [PubMed: 16890988]

Wang Y, Volloch V, Pindrus MA, et al. Murine osteoblasts regulate mesenchymal stem cells via WNT and cadherin pathways: mechanism depends on cell-cell contact mode. J Tissue Eng Regen Med. 2007; 1(1):39–50. [PubMed: 18038391]

Wozney JM. The bone morphogenetic protein family and osteogenesis. Mol Reprod Dev. 1992; 32(2): 160–167. [PubMed: 1637554]

Yamaguchi A, Katagiri T, Ikeda T, et al. Recombinant human bone morphogenetic protein-2 stimulates osteoblastic maturation and inhibits myogenic differentiation *in vitro*. J Cell Biol. 1991; 113(3): 681–687. [PubMed: 1849907]

Yoneda T, Hiraga T. Crosstalk between cancer cells and bone microenvironment in bone metastasis. Biochem Biophys Res Commun. 2005; 328(3):679–687. [PubMed: 15694401]

Yonou H, Yokose T, Kamijo T, et al. Establishment of a novel species- and tissue-specific metastasis model of human prostate cancer in humanized non-obese diabetic/severe combined immunodeficient mice engrafted with human adult lung and bone. Cancer Res. 2001; 61(5):2177–2182. [PubMed: 11280783]

Zhang J, Dai J, Qi Y, et al. Osteoprotegerin inhibits prostate cancer-induced osteoclastogenesis and prevents prostate tumor growth in the bone. J Clin Invest. 2001; 107(10):1235–1244. [PubMed: 11375413]

Zhu H, Mazor M, Kawano Y, et al. Analysis of *Wnt* gene expression in prostate cancer: mutual inhibition by WNT11 and the androgen receptor. Cancer Res. 2004; 64(21):7918–7926. [PubMed: 15520198]

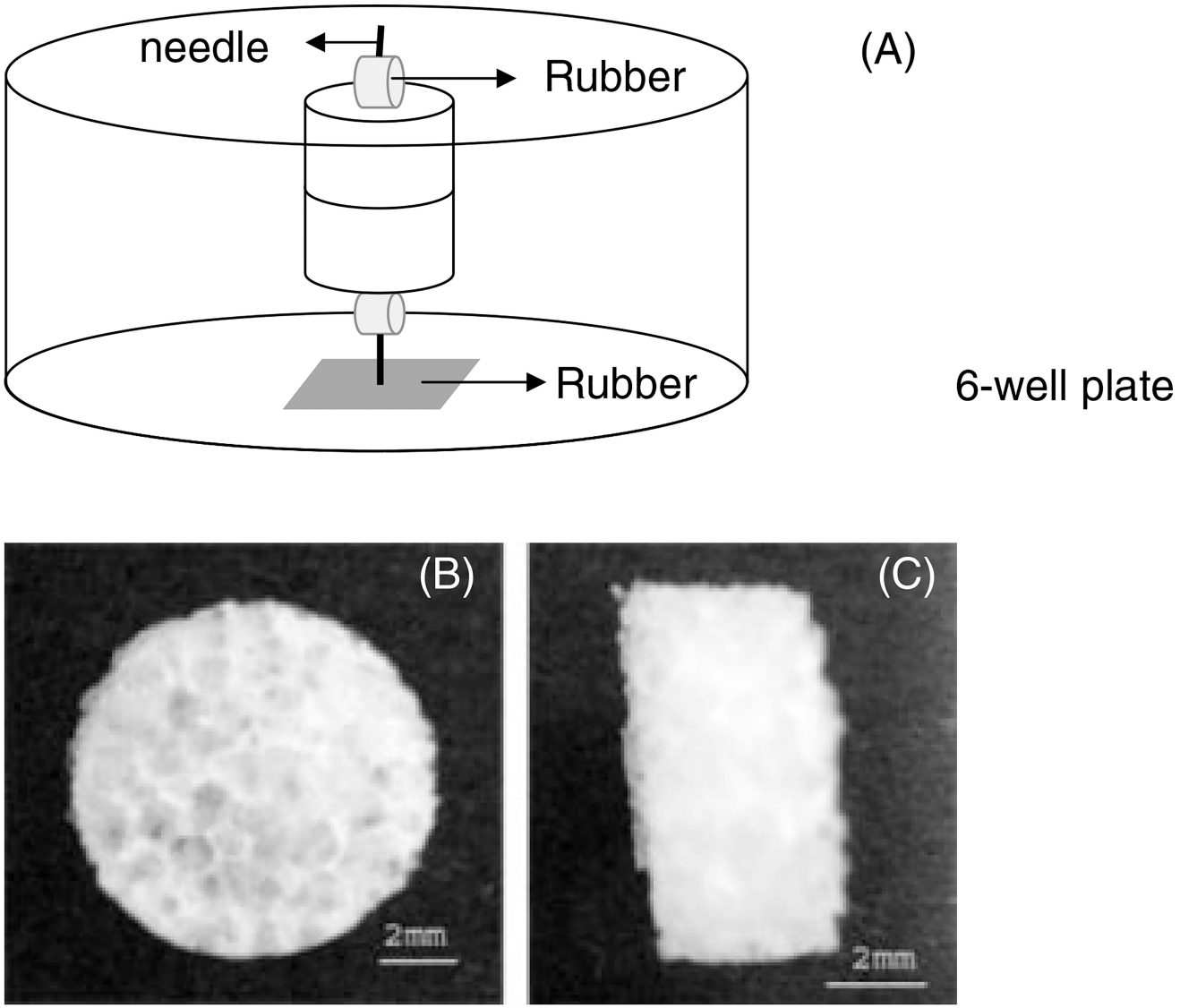

Figure 1.

Design of a 3D model system *in vitro* and 3D porous aqueous-based scaffold (pore size, 1000–1180 μm). (A) Two scaffolds were attached, fixed using a needle and rubber mat to stabilize them in medium. (B, C) 3D porous aqueous-based silk scaffold cut to size 8 × 3 mm (diameter × height). Scale bar = 2 mm

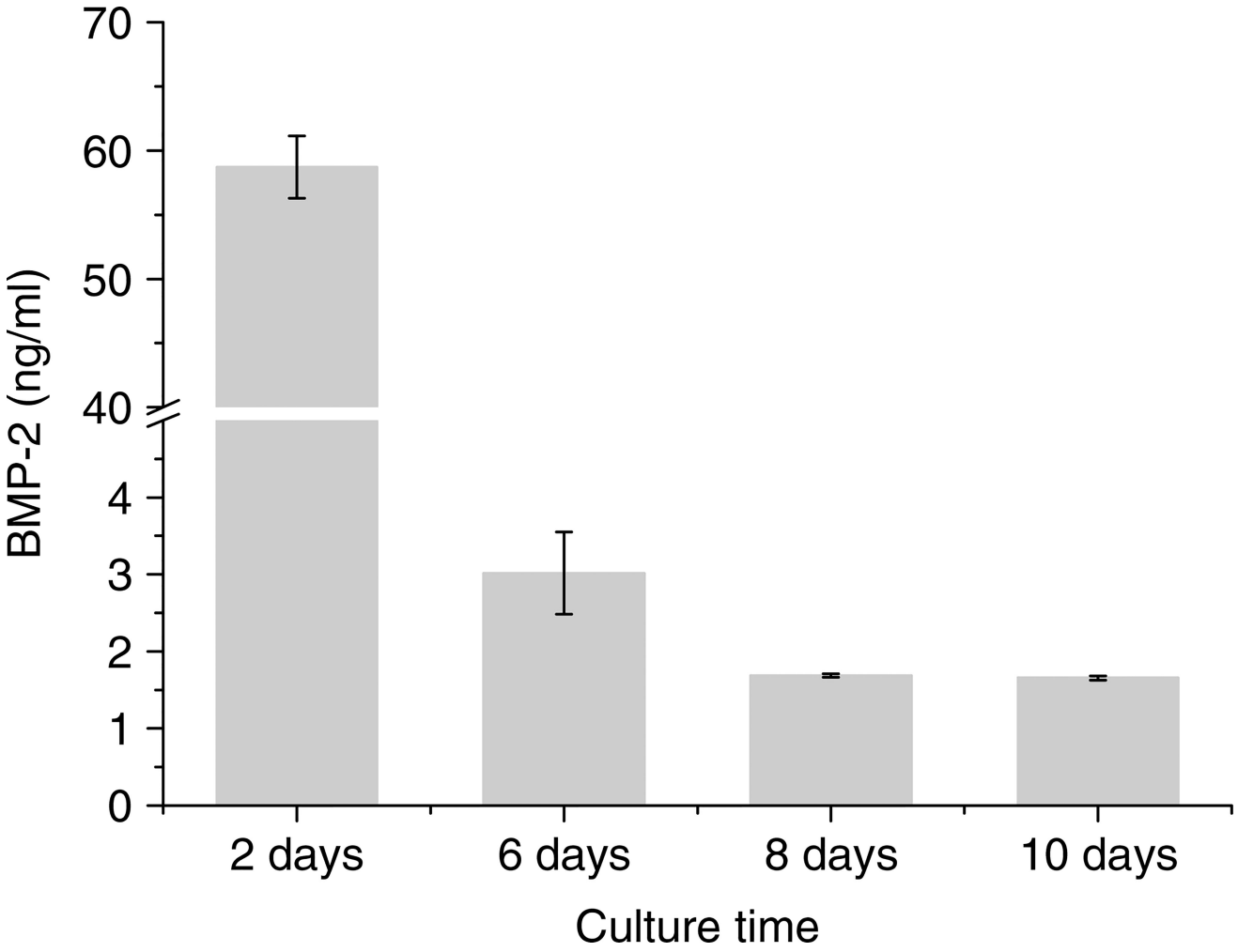

Figure 2.
Quantification of BMP-2 in medium recovered from the scaffolds by ELISA. 30 μg BMP-2 was covalently coupled onto each scaffold

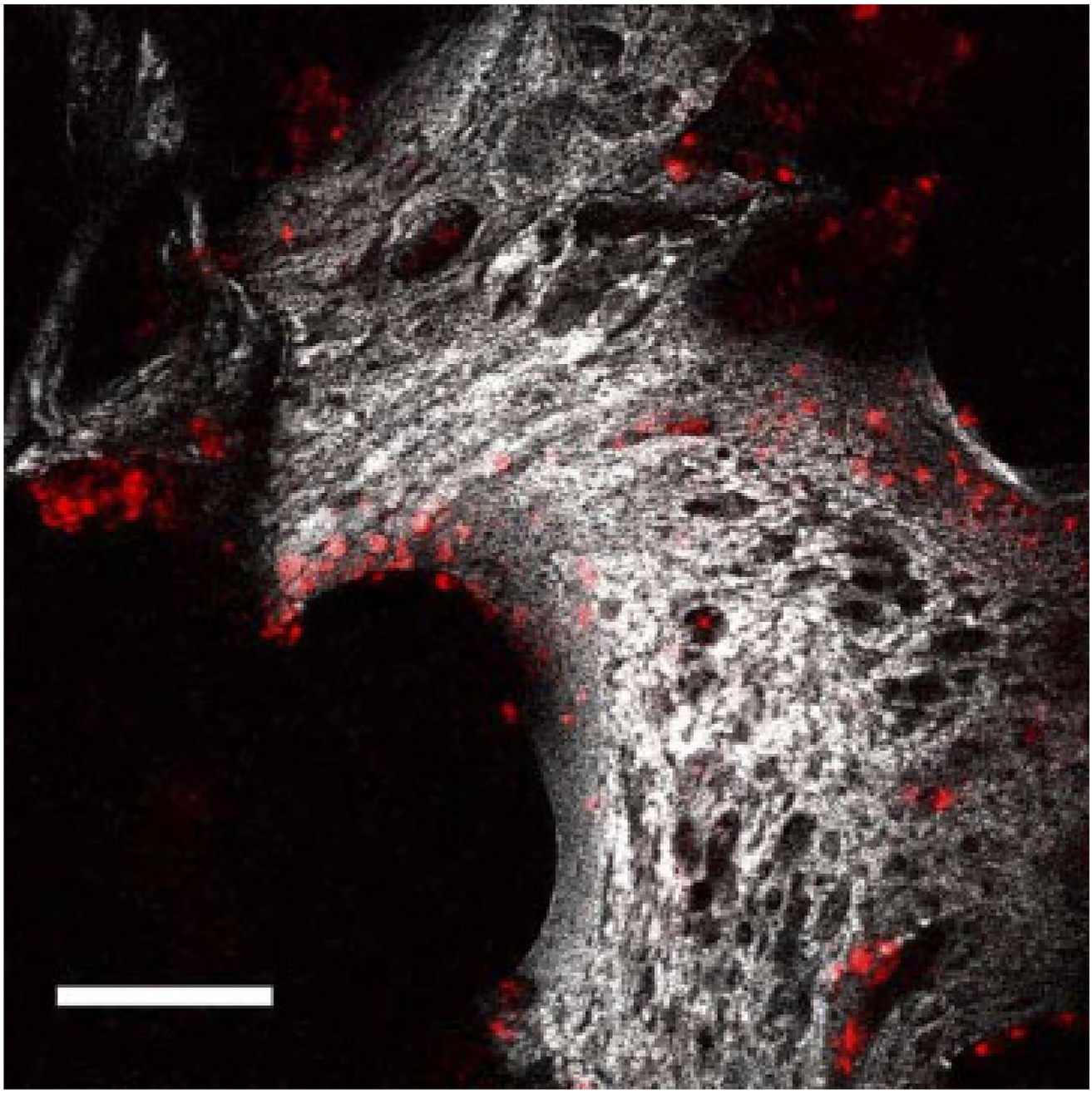

Figure 3.
Projections of composite single and two photon-excited fluorescence image stacks of PC3 on silk scaffold taken over approximately 155 μm. PC3 cells were labelled with DiI (red colour; Ex, 543 nm, Em, 550–575 nm). Scale bar = 150 μm

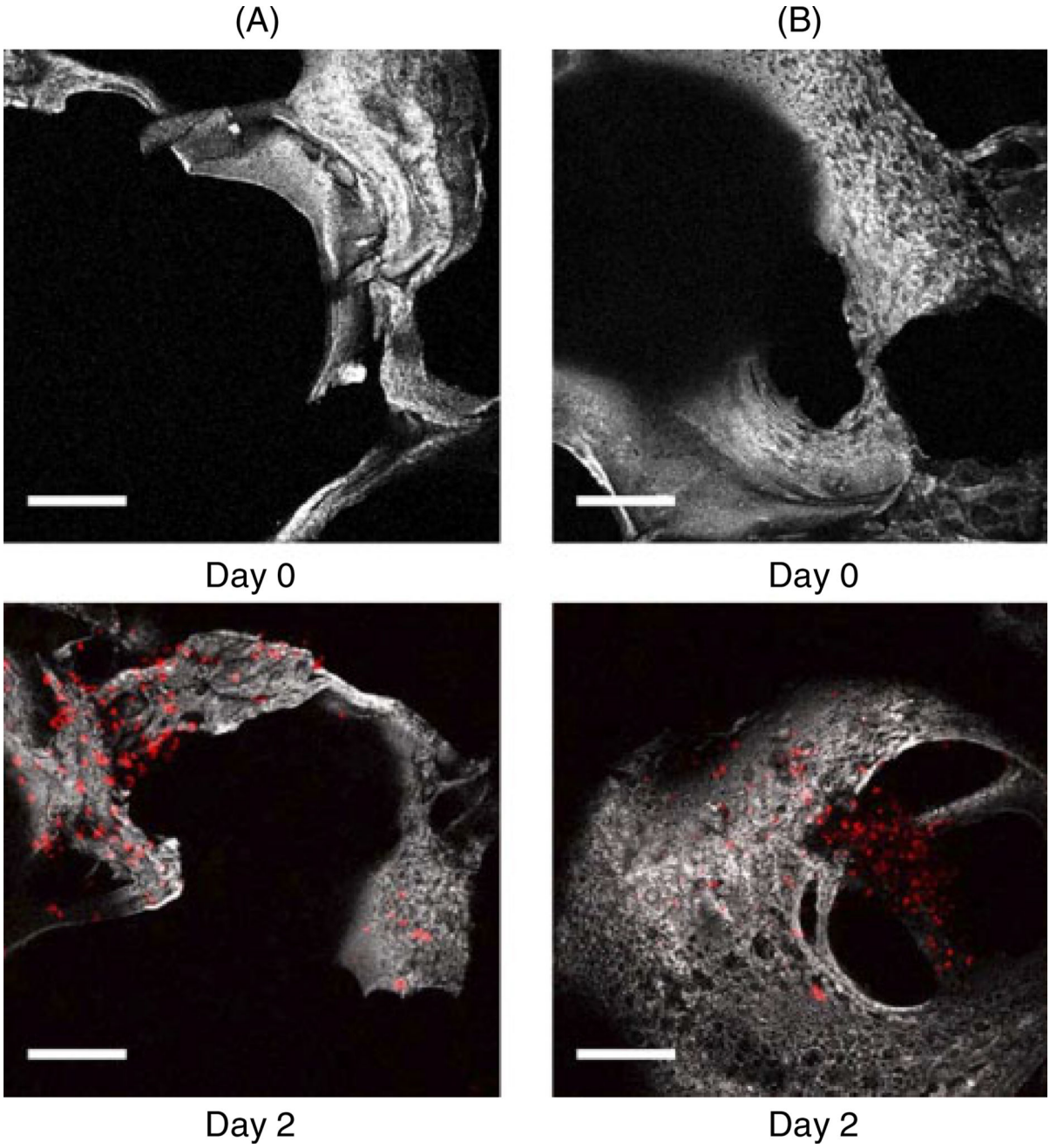

Figure 4.

Projections of composite single and two-photon excited fluorescence image stacks of (A) unmodified scaffolds and (B) BMP-2-coupled scaffolds, taken over a total depth of approximately 155 μm. Scale bar = 150 μm

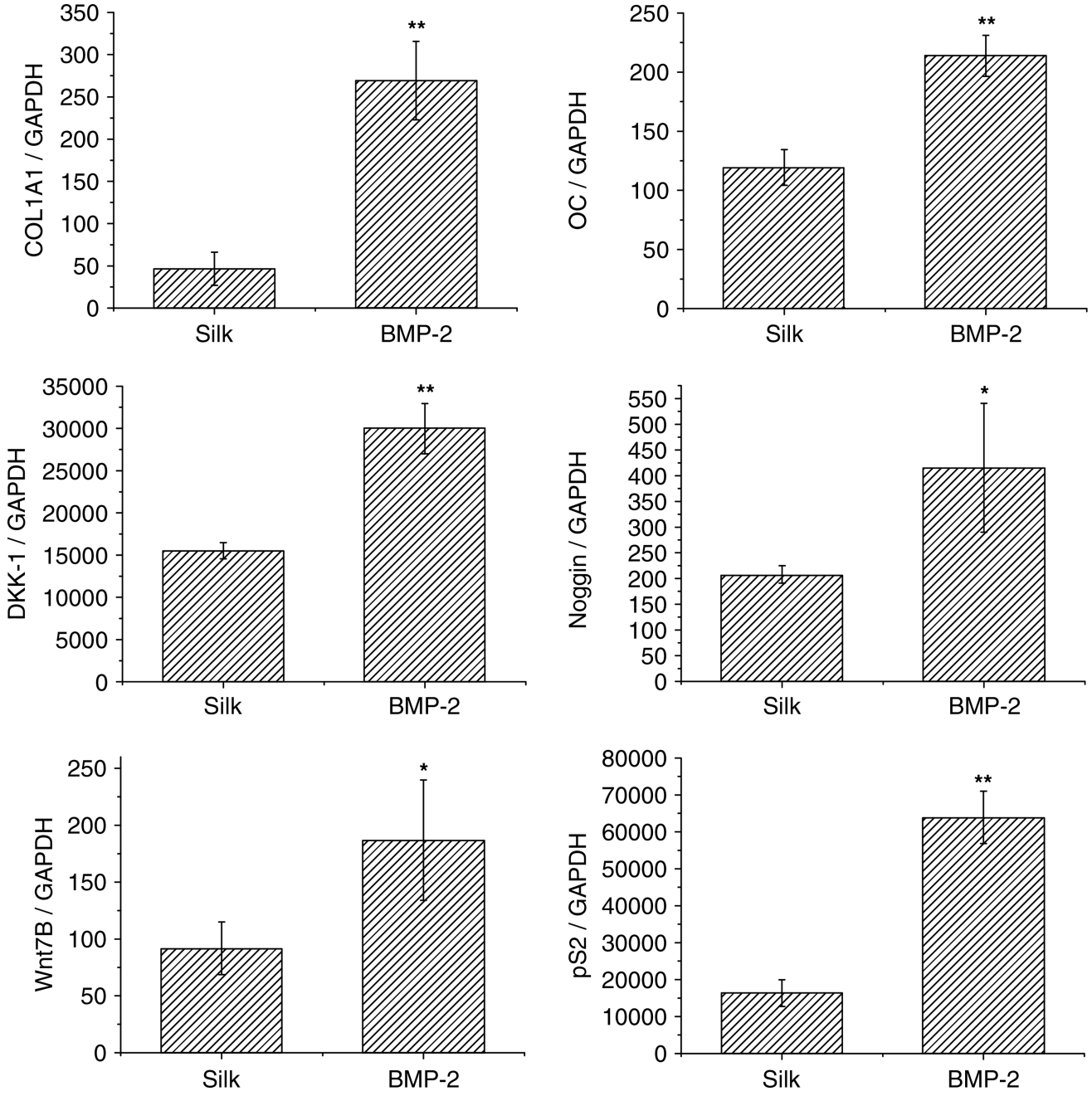

Figure 5.

Gene expression in the bottom scaffolds; unmodified scaffolds (silk) and BMP-2-coupled scaffolds (BMP-2). Transcript levels were quantified by qPCR and normalized to GAPDH. *$p < 0.05$, **$p < 0.01$, statistically significant differences

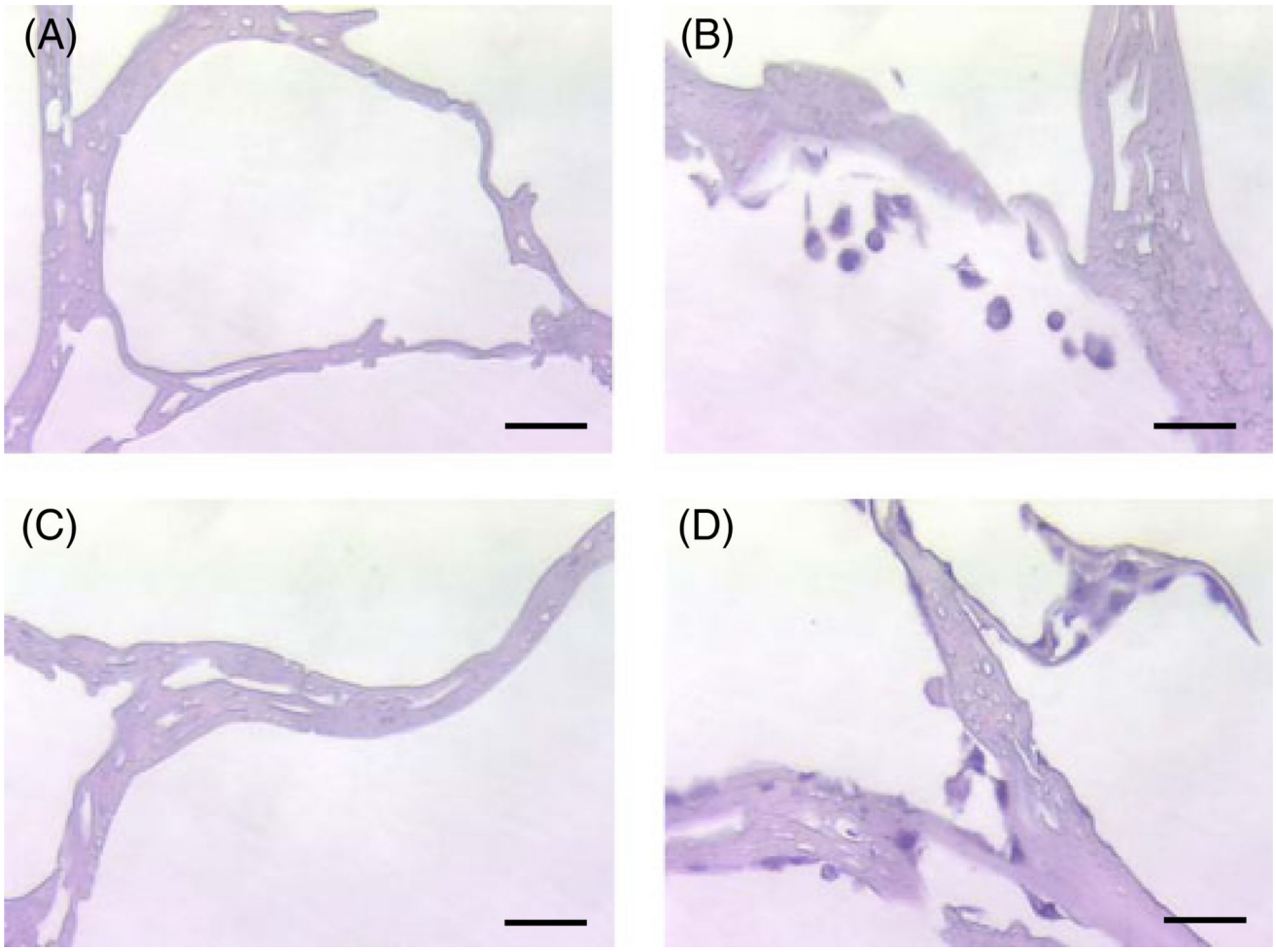

Figure 6.
H&E staining of cross-sectioned bottom scaffolds. (A, B) Unmodified scaffolds; (C, D) BMP-2-coupled scaffolds. Scale bar = 50 μm

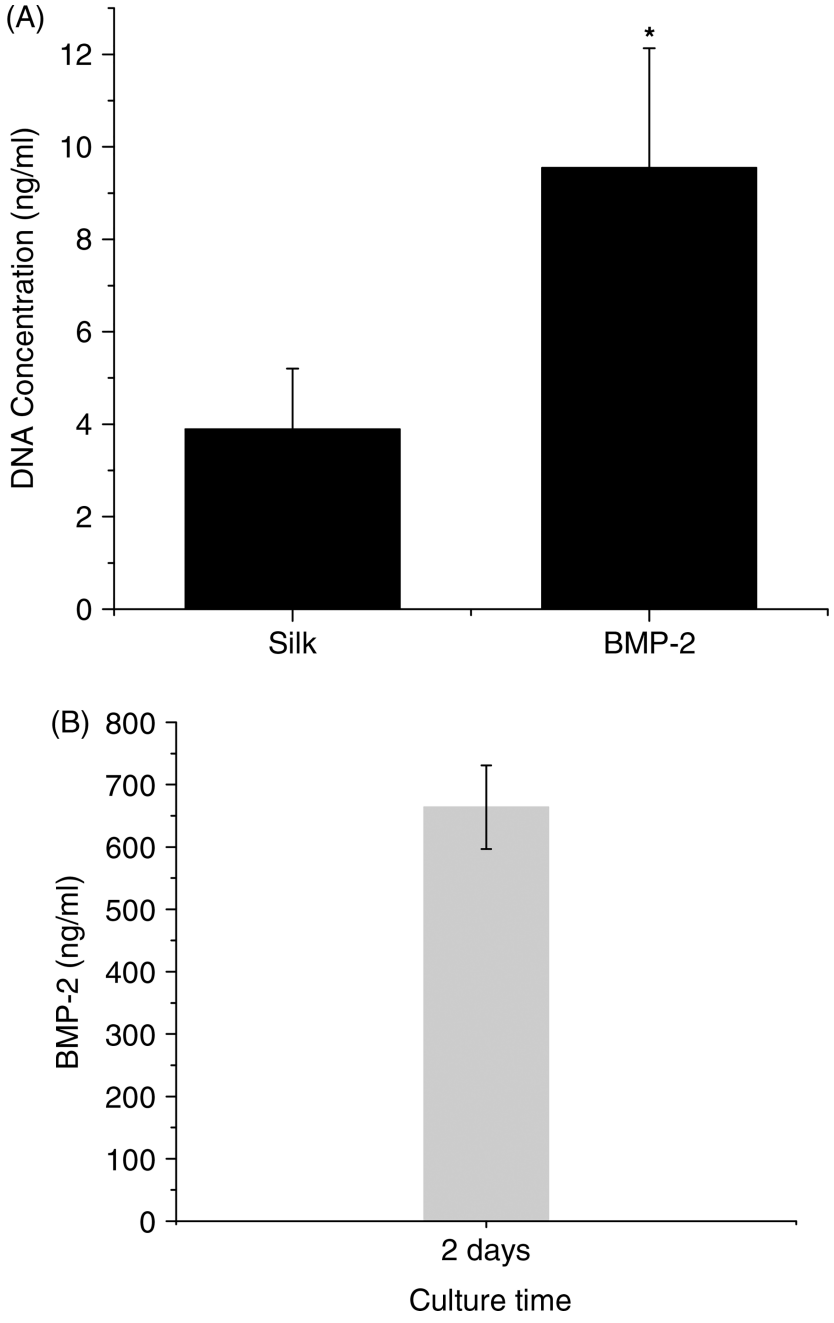

Figure 7.

Biochemical analysis of the top scaffolds. (A)The migration of PC3 cells to the top scaffolds was determined by DNA content in the scaffolds. (B) BMP-2 concentration recovered from the scaffolds was quantified by ELISA. 30 μg BMP-2 was covalently coupled onto each scaffold